Development of Functional Material for anti-Counterfeiting and Authenticity Verification of Ceramic Products

Masaki Fujikawa, Mariko Hara, Yasushi Nanai, and Shingo Fuchi

***Abstract*—This study introduces a functional material called glass phosphor, which emits both visible and near-infrared spectra via optical excitation using 980-nm light. This glass phosphor exhibits both up and down conversions while receiving only one excitation light. This transparent, harmless, and pale pink material has affinity with the glassy layer of a ceramic product, and the ceramic product's patterns and colors remain unaffected when a small amount of phosphor powder is welded onto its surface. After the powder had been welded, four types of optical feature data were extracted from the ceramic product and used to verify its authenticity. Because the genuine product's hue, emission intensity and the light path generated by the glass phosphor particles are hard to replicate, the powder of this material could be used for anti-counterfeiting of the genuine product.**

***Index Terms*—Anti-counterfeiting, authentication, glass phosphor, optical feature information, up and down conversion.**

I. Introduction

A. Background and Target

A ceramic product prepared by a renowned potter or bearing the brand of a famous manufacturer is popular among customers and likely to be traded with a high price tag as a luxury item. A counterfeiter of ceramics creates a copy while observing a genuine product and sells it to a customer or antiquarian with poor appraisal skills [1]. Distribution of copied products on the market causes problems for genuine ceramic artists or manufacturers and the customer, which includes violating the pottery's or brand's intellectual property rights and costing them their revenue essentially obtainable upon their business and giving mental and monetary damages to buyers those who wrongly purchased the copied product; hence, counterfeiting should not be overlooked.

We have been attempting to create a better method of mechanically verifying the product's authenticity with high accuracy so that a buyer with low appraisal skills does not purchase a copied product unknowingly. Because the proposed method also makes it difficult to create a clone of a genuine product, it is part of the anti-counterfeiting techniques called artifact metrics [2]. In our previous research paper [3], we considered a transparent, pale blue functional material called glass phosphor that emits one peak wavelength of near-infrared light via optical excitation and proposed the idea of welding a small amount of phosphor powder onto the surface of a ceramic product. The features of this method are as follows.

1) Because glass phosphor is harmless, it does not negatively affect the human body or the environment. Owing to its pale color and transparency, welded phosphor powder does not affect the product's patterns or the colors depicted on the surface of the product.
2) Feature information (photos with emissions from phosphor powder captured by an indium gallium arsenide near-infrared camera), used to verify the product's authenticity, can be extracted from the product without contact.
3) Even if counterfeiters manage to acquire glass phosphor, replicating the genuine product's hue, emission intensity, and the light path generated by the phosphor particles scattered on the surface of the product is optically quite difficult, rendering the counterfeiting of the products quite difficult.

Borrowing from multimodal biometrics [4], a method of identifying individuals by using several biometric details (such as fingerprint, retina, and vein pattern), a technique called multimodal artifact metrics was proposed to improve the accuracy of authentication and the difficulty of counterfeiting by extracting multiple optical feature details from an artifact [5]. Although we have previously focused on creating a better method of applying this technique to the ceramic product and extracting multiple optical feature details from it, herein, we describe a new glass phosphor that could achieve this technique. This paper is organized into five sections. In this section, we summarize artifact metrics and multimodal artifact metrics. In Section II, we describe the concept of the glass phosphor and the feature information possibly extracted from a ceramic product with welded phosphor particles. In Section III, development of the glass phosphor and experimental results are described. We describe our considerations in Section IV and conclude this paper in Section V.

B. Summary of the Artifact Metrics

The concept of the artifact metrics derives from biometrics.

Manuscript received May 15, 2019; revised July 16, 2019. This work was supported by JSPS KAKENHI Grant Number 18K11302 and The Kazuchika Okura Memorial Foundation.

Masaki Fujikawa is with Kogakuin University, Hachioji, Tokyo 192-0015 Japan (e-mail: fujikawa@cc.kogakuin.ac.jp).

Mariko Hara was with Kogakuin University. She is now with DTS Corporation, Chuo-ku, Tokyo 104-0032 Japan.

Yasushi Nanai and Shingo Fuchi are with Aoyama Gakuin University, Sagamihara, Kanagawa Pref., 252-5258 Japan.

doi: 10.18178/ijmmm.2019.7.4.451

Each artifact has unique characteristics. An artifact's authenticity can be verified by extracting characteristic information from the target artifact and comparing it with the registered feature information. The greater the similarity, the higher the degree of authentication. The difficulty of counterfeiting is established based on technological evidence, by which the characteristic information held by the genuine product is difficult to copy. This characteristic information is formed spontaneously and randomly during the manufacturing process, and cannot be formed intentionally even by manufacturers of genuine products. Hence, the difficulty of counterfeiting cannot be decreased if the mechanism of forming characteristic information is accessible to the public.

Microscopically, each artifact has different characteristic information, such as tiny roughness and color shade. However, specifying the area photographed by registration phase and the area shot by verification phase is time consuming, because the area observed using a microscope is quite small [3]. Hence, in artifact metrics, a method is utilized to form unique and easy-to-extract characteristic information in the artifact [3]-[6]. Specifically, additives having physical features are added during the manufacturing process. The particles are distributed randomly and fixed in the artifact. The distribution degree reflects the characteristic information. Sensing devices which can extract the physical features of additives are used when extracting characteristic information.

TABLE I: PHYSICAL CHARACTERISTICS AND EXTRACTED FEATURE INFORMATION

Physical characteristics	Extracted feature information
Optical characteristics	Particles' optical characteristics (reflection, transmission, infraction, and fluorescence) and their degree of distribution reflect the characteristic information, which is extracted by sensors that can detect light intensity.
Magnetic characteristics	Particles' magnetic characteristics (attraction and repulsive force) and their degree of distribution reflect the characteristic information, which is extracted by sensors that can detect a change in magnetism.
Electrical characteristics	Particles' electric characteristics (electrical charge) and the degree of distribution reflect the characteristic information, which is extracted by sensors that can detect the quantity of electric charge.
Vibration characteristics	Particles' vibration characteristics (sonic waves) and the degree of distribution reflect the characteristic information, which is extracted by sensors that can detect sonic waves.

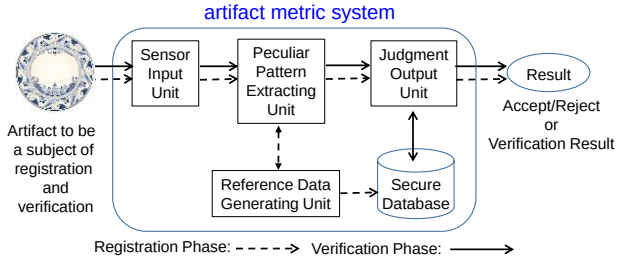

Fig. 1. Artifact metric system (Image).

Table I shows the physical characteristics of materials added in the manufacturing process and the characteristic information extracted from them. Fig. 1 shows an overview of the system (artifact metric system) that uses artifact metrics. Two phases depicted as straight and dashed lines are almost the same as those of biometrics. In this system, characteristic information that is extracted from each artifact before it is shipped is stored in a secure database. To verify the authenticity of an artifact, the system extracts the characteristic information from it and compares the information with that of the registered feature in the secure database.

TABLE II: COMPARISON BETWEEN TWO APPROACHES

	Approach 1	Approach 2
Advantages	Low probability of affecting the artifact's moldability and physical strength.	Increases the number of extractable feature information.
Drawbacks	Limited with regard to the number of extractable feature information.	High probability of affecting the artifact's moldability and physical strength.

C. Summary of the Multi-modal Artifact Metrics

Characteristic information extracted from artifacts can be changed, depending on environmental situations during extraction (such as temperature, humidity, and position of artifacts relative to sensing devices). However, even in such situations, the artifact metric system should be able to verify authenticity stably and correctly, using the strong correlation between the characteristic information registered in the database and the information features extracted during verification.

There is an approach to increase the number of characteristic information to find strong correlations between both registered and extracted information [3]. This approach is named "multi-modal artifact metrics [5]" because various characteristic information is used.

This approach can be further categorized into two methods. The first one (approach 1) focuses on additives having one physical feature and extracts two or more types of characteristic information from the artifact. For example, in our previous paper [3], especially in the "consideration" section, we focused on the optical feature of glass phosphor and proposed another idea to utilize two distributions (emission spectrum and emission intensity distribution) as the characteristic information. These distributions can reflect the particle size and degree of dispersion of glass phosphor welded on the surface of ceramic products.

The second method (approach 2) adds two or more additives having different physical features to the artifact, from which two or more types of characteristic information can be extracted. For example, in our previous study [5], we proposed an idea of creating thin films inside synthetic resin cards (used for valuable cards) using a conductive polymer paint having electrical features, and infrared up-conversion phosphor powder having optical features. This method utilizes emission intensity and sheet resistance which reflect the size and dispersion of phosphor particles in thin films. This information could be used as the characteristic information.

The differences of both methods are listed in Table. II. Although approach 1 is limited by the amount of

characteristic information extracted from the artifact, it could reduce the quantity of materials for the total amount of artifacts. Approach 2 could increase more characteristic information than the former one. However, it could also affect the artifact's moldability and physical strength, because the material quantity for the total amount of artifacts increases.

In this paper, we develop and use a new glass phosphor with a unique optical feature. Our method corresponds to multimodal artifact metrics approach 1, because we intend to extract multiple feature details from a ceramic product with welded glass phosphor particles.

II. Design of the Grass Phosphor

A. Concept

To realize our idea of extracting multiple optical feature details from a ceramic product, we developed a new, harmless, transparent, and pale glass phosphor. This phosphor emits three peak wavelengths by a single optical excitation wavelength (Fig. 2). Two peaks are in the visible spectrum, and one peak exists in the near-infrared spectrum.

This phosphor emits two emission peak wavelengths (red and green bands) in the visible spectrum and one emission peak wavelength (near 1500 nm) in the near-infrared spectrum. The up-conversion phenomenon means that the emission can be seen on the side of a wavelength shorter than the excitation light wavelength, whereas a down-conversion phenomenon shows the opposite emission (it can be seen on the side of a longer wavelength). As shown in Fig. 2, this glass phosphor shows both up- and down-conversion phenomena while receiving one excitation light at 980 nm.

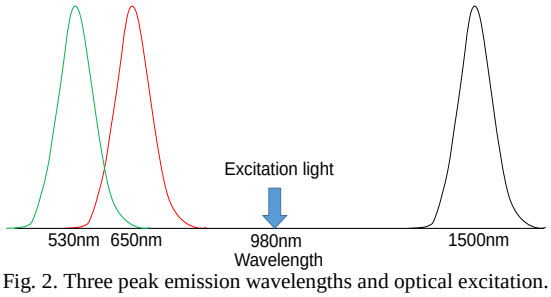

Fig. 2. Three peak emission wavelengths and optical excitation.

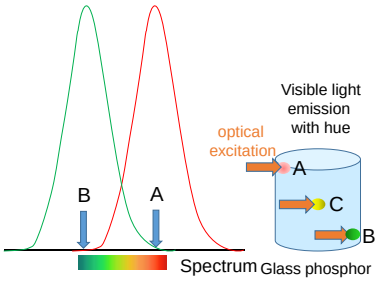

Fig. 3. Two peak emission wavelengths and emission image on the glass phosphor (in the visual spectrum).

Fig. 3 shows an emission image of the glass phosphor in the visible spectrum. The phosphor is emitted when it receives the excitation light, but the hue and emission intensity vary at the point eradiated by the light. For example, in Fig. 3, red with weak emission intensity is observed at point A, whereas green with strong emission intensity can be seen at point B on the surface of the phosphor. If yellow with moderate emission intensity is observed at point C, it means that two colors (red and green) with similar emission intensities are generated by optical excitation.

The phosphor also brings different emission intensities in the near-infrared band (Fig. 4). For example, a low emission intensity of near-infrared light is observed at point A (red in Fig. 3), whereas a strong emission intensity of near-infrared light can be seen at point B (green in Fig. 3) on the surface of the phosphor. In this figure, a moderate emission intensity of near-infrared light is observed.

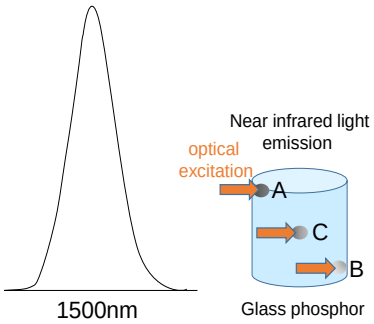

Fig. 4. One peak emission wavelength and emission image on the glass phosphor (in the near infrared spectrum).

B. Rare Earth Oxide and Three Emission Peak Wavelengths

To develop the glass phosphor shown in Fig. 2, we use two rare earth oxides: ytterbium oxide (Yb_2O_3) and erbium oxide (Er_2O_3). Yb_2O_3 absorbs the excitation light with a 980-nm near-infrared light and transmits the light energy to erbium (Er) ions as excitation energy. In contrast, the Er ion emits red and green (in the visible spectrum) and near-infrared light (near 1500 nm).

C. Two Ions and the Emission Difference

The emission difference shown in Fig. 3 and Fig. 4 could be generated because of differences in the numbers of ytterbium (Yb) and Er ions and the distances between them. The reason for these differences is unevenness of both ions in the glass phosphor. This unevenness could be generated spontaneously during the synthesis process in the furnace (while melting rare earth oxides) and generate points in the glass phosphor where the numbers of Yb and Er ions and the distances between them are uneven.

The emission hue and emission intensity in the visible spectrum can be changed by the distance between ions and the ratio of the numbers of Yb and Er ions. However, the emission intensity in the near-infrared spectrum (near 1500 nm) was controlled by the number of Er ions.

In general, a phosphor that shows a peak wavelength in the visible spectrum or near-infrared spectrum by optical excitation (with near-infrared light) is developed with the goal of one sharp peak wavelength (or a single light emission). Developers of phosphor are likely to avoid a situation in which the phosphor emits uneven color. However, in our study, we used this situation subtly to take advantage of it.

So far, developing an up- and down-conversion phosphor with three peak wavelengths with single excitation light (shown in Figs. 3 and 4) by changing the ratio of rare earth

oxides has been rarely reported. An approach exists for developing glass phosphor with the same features (shown in Fig. 3 and Fig. 4) using an ultraviolet (UV) light source. However, UV light could deteriorate the pigment and affect the colors or the pattern of the ceramic during irradiation on the surface of products [7]. Hence, we do not adopt this approach.

D. Extractable Feature Information

If the glass phosphor, which shows emissions as indicated in Fig. 3 and Fig. 4, was welded onto the surface of the ceramic product, four types of optical feature data could be extracted from the product while excitation light at 980 nm was irradiated. The first type, introduced in our previous papers [3], [8], [9], is an image captured by a visible light camera and an infrared light camera (Fig. 5 shows example images). This information could be obtained from the product with no contact.

The remaining three types of feature data are related to the emission intensity. We explained earlier that the emission difference could be observed at each observation point while it receives the excitation light. Fig. 6 shows the relationship between this phenomenon and the remaining three types of feature data. Fig. 6 depicts the emission intensities of point X and point Y (each point was irradiated by the excitation light at 980 nm, and each emission intensity was observed by a spectroscope with no contact). We assume that the parameters *Rx*, *Gx*, and *Nx* were observed at point X and the parameters *Ry*, *Gy*, and *Ny* were captured at point Y. *Rx* and *Ry* are the maximum values of emission intensity in the red band. Likewise, *Gx* and *Gy* are the maximum values of emission intensity in the green band, and *Nx* and *Ny* are the maximum values of emission intensity in the near-infrared spectrum. Using this, the remaining three types of feature data at point X could be determined as follows:

1) Emission intensity: Each emission intensity at point X could be observed for each light band and the near-infrared spectrum, such as *Rx*, *Gx*, and *Nx*.
2) Emission intensity ratio 1: Parameter *Lx_max* could be determined as the total value of the light observed by the spectroscope at point X. Then, each ratio (*Rx* to *Lx_max*, *Gx* to *Lx_max*, and *Nx* to *Lx_max*) could be feature data.
3) Emission intensity ratio 2: The ratio of each emission intensity could be feature data, such as *Rx* to *Gx*, *Gx* to *Nx*, and *Rx* to *Nx*.

Because the feature information could be increased from that found in our previous research [8], [9], we predict that this feature information could contribute to improving the accuracy of authentication and the difficulty of counterfeiting.

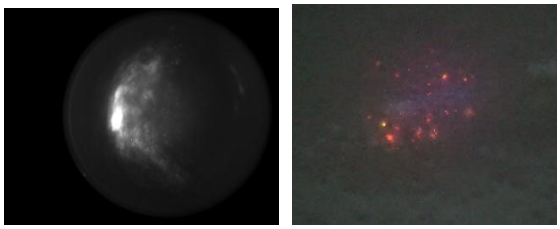

Fig. 5. Emissions captured by a near-infrared camera (left) and by a visual light camera (right).

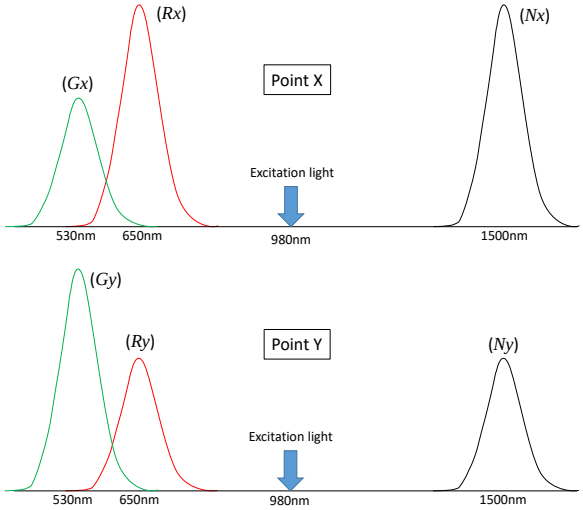

Fig. 6. Difference in emission intensity of each observation point irradiated by excitation light (top: point X, bottom: point Y).

E. Welding Glass Phosphor Powder

To be able to extract the four types of feature data described in the previous section from the ceramic product, we pulverized the grass phosphor and welded it onto the surface of the product in the furnace, as done in our previous studies [3], [8], [9]. Welding phosphor powder (or retaining the unevenness of the phosphor particles while welding) leads to unevenness in the ratio of the two ion numbers and of the distance between them. Hence, the emission differences shown in Fig. 3 and Fig. 4 could be seen at each observation point eradiated by the excitation light.

III. Experiments

A. Making Base Glass Material

In general, the glass phosphor can be made by melting a mixture of rare earth oxide and base glass material in a furnace. Both materials in a crucible are melted at 1230 °C for 20 minutes. After pulling the crucible from the furnace, the melted material is cooled on a mold made of metal. Because the amount of rare earth oxide against the base glass material is low, to make transparent and pale glass phosphor, the base glass material should have more transparency and less color.

Based on previous research findings [8], [9], we reviewed the composition of the base glass material — in particular, a glass-forming oxide and a glass-modifying oxide. These oxides form the base glass material. Before choosing candidate materials, we set the following conditions:

1) The candidate material should be colorless. In general, glass-forming oxide and glass-modifying oxide are provided as powder, so their color is likely to be white because of light scattering. Hence, white oxide should be chosen.
2) The melting point should be below 1400 °C. This is because the glass phosphor should be melted completely in the furnace at a temperature of 800–1300 °C so that it can be welded onto the surface of the ceramic product.

We selected the following five oxides as candidate

materials based on the preceding conditions:

TABLE III: COMPONENT OF THE BASE GLASS MATERIAL

No.	Composition	No.	Composition
1	GeO_2	4	GeO_2-Sb_2O_3
2	TeO_2	5	GeO_2-MoO_3
3	Sb_2O_3	6	GeO_2-Li_2CO_3

(a) Germanium oxide (GeO_2)
(b) Tellurium oxide (TeO_2)
(c) Antimony oxide (Sb_2O_3)
(d) Molybdenum oxide (MoO_3)
(e) Lithium carbonate (Li_2CO_3)

We made samples of base glass material based on the combinations shown in Table III. In this table, combinations Nos. 1–6 are not round robin (or all combinations of the candidate oxides). We created six combinations for the following reasons:

- No. 1 (GeO_2) is called a glass-forming oxide. Glass can be formed by GeO_2 only.
- No. 2 (TeO_2) and No. 3 (Sb_2O_3) are classified as glass-modifying oxides and have a high potential of forming glass. We intended to test each oxide's potential for forming glass without other oxides.
- For No. 4 (GeO_2-Sb_2O_3), we consider Sb_2O_3 to be a modifying oxide. We intended to test whether glass could be formed with a mixture of Sb_2O_3 and GeO_2, a glass-forming oxide.
- For Nos. 5 (GeO_2-MoO_3) and 6 (GeO_2-Li_2CO_3), it is obvious that glass cannot be formed, because MoO_3 and Li_2CO_3 are modifying oxides and they do not have the potential to form glass. Hence, we intended to test whether glass could be formed by mixing either of these oxides with GeO_2, a glass-forming oxide.

The results of the experiment showed that base glass material made from No. 6 (75 GeO_2-25 Li_2CO_3) had the highest transparency and least amount of coloration (Fig. 7).

This base glass material contains Li_2CO_3, and it has hygroscopicity. If Li_2CO_3 was used as a material for making glass, it could absorb moisture in the air, so the appearance of the glass could lose its transparency and the color could be whitish. Addressing this concern, we exposed the base glass material to air over 10 months and observed its appearance. However, the appearance did not show changes. We assumed that the characteristic of Li_2CO_3 (moisture absorption) is no longer present because the material underwent vitrification.

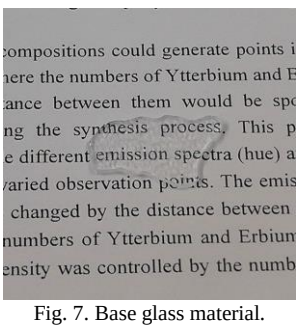

Fig. 7. Base glass material.

TABLE IV: RATIO OF RARE EARTH OXIDE

No.	1	2	3	4	5	6
Yb_2O_3	1.0	1.0	1.0	2.0	2.0	2.0
Er_2O_3	0.07	0.1	0.13	0.05	0.07	0.1
No.	7	8	9	10	11	12
Yb_2O_3	2.0	3.0	3.0	3.0	3.0	3.5
Er_2O_3	0.13	0.03	0.07	0.1	0.13	0.07
No.	13	14	15	16		
Yb_2O_3	3.5	4.0	5.0	5.0		
Er_2O_3	0.1	0.06	0.07	0.08		

The base glass material and the glass phosphor should be stable for a long period, so we observed the appearance of the base glass material continuously.

B. Making Glass Phosphor

Because the component of the base glass material was determined, we conducted another experiment to confirm whether the glass phosphor, described in Section II, could be made. In Table IV, we show the ratio of Yb_2O_3 and Er_2O_3 to be mixed with the base glass material. In our previous research [9], glass phosphor with the ratio of No. 9 (3.0 Yb_2O_3-0.07 Er_2O_3) showed emission as illustrated in Fig. 3 and Fig. 4. Hence, we set ratios from Nos. 1–16 to observe the emission from candidate glass phosphor made with these ratios. We also set the weight of the glass phosphor samples to be 5 g for consistency with our previous research [9].

First, we found a point on each sample of the glass phosphor that shows the strongest emission while irradiating excitation light at 980 nm.

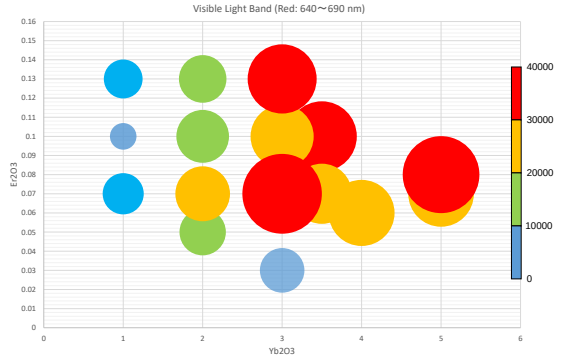

Fig. 8. Integrated emission intensity in visible light band (red light).

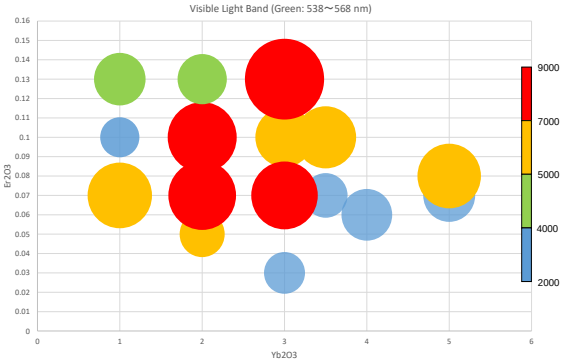

Fig. 9. Integrated emission intensity in visible light band (green light).

Next, we measured the emission spectrum at that point

using a spectroscope and calculated the point's integrated value of the emission intensity. This value is depicted using graphs in Figs. 8–10. Fig. 8 shows the integrated value of each point of the samples in the red light band (from 640 to 690 nm). Fig. 9 shows the same points of integrated values in the green light band (from 538 to 568 nm). Fig. 10 shows the same points of integrated values in the near-infrared spectrum (from 1435 to 1689 nm). The more the circle expands, the stronger a point's emission intensity. Red indicates the emission intensity was strong, whereas blue means it was weak.

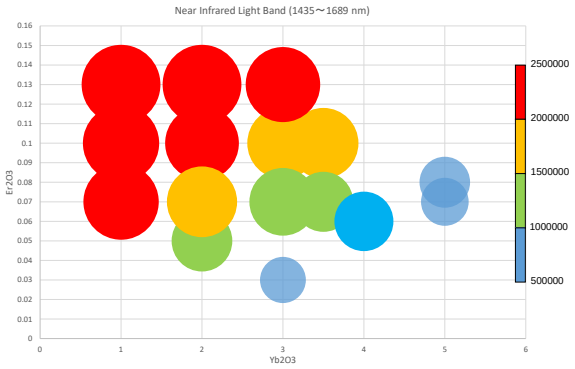

Fig. 10. Integrated emission intensity in near infrared light band.

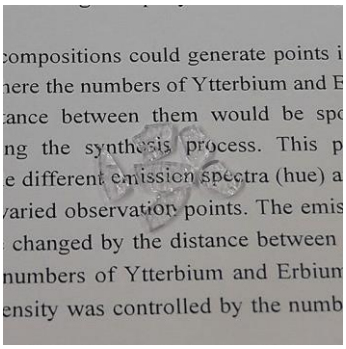

Fig. 11. Glass phosphor.

The graphs show that each sample emitted in each light band, but that sample No. 11 showed strong emission in each band. Fig. 11 shows the glass phosphor with the ratio 3.0 Yb_2O_3-0.13 Er_2O_3. Compared with Fig. 7, the appearance of this phosphor is pale pink, derived from Er, but the coloration is pale and transparent.

IV. Considerations

A. Safety of Glass Phosphor

In general, glass phosphor is formed by rare earth oxide and glass-forming oxide. First, we describe the safety of the oxides we used in our experiment.

We used Er_2O_3 and Yb_2O_3 as a rare earth oxide. According to experts, rare earth does not show obvious toxicity [10]. We used Li_2CO_3 as a glass-modifying oxide and GeO_2 as a glass-forming oxide. Li_2CO_3 is used as an additive or agent not only for medicine but also for heat-resistant ceramics and glass [11], so it seems to be safe. GeO_2 does not show obvious toxicity to humans and environment [12].

TABLE V: Usage of each Reagent, Weight, and Market Price

Name	Used amount (grams)	Weight/Bottle (grams)	Price/Bottle (USD)
Yb_2O_3	0.618	25	523.75
Er_2O_3	0.026	25	402.88
GeO_2	3.976	25	145.04
Li_2CO_3	0.936	25	10.65
Total amount	5.556		

Next, we describe the safety of the glass phosphor.

The glass phosphor is a compound of the rare earth oxide and base glass material. It is incombustible, insoluble, and chemically stable oxide glass [3].

Based on these descriptions, the rare earth oxides, modifying oxides, and glass phosphor made from these materials are considered safe and have a low risk of affecting human health and the environment. However, care should be taken to prevent inhalation and adhesion of the particles to unprotected eyes while handling the powders.

B. Monetary Cost of Making Glass Phosphor

Table V shows the amounts of rare earth oxides and modifying oxides used to make 5 g of the glass phosphor. Each amount comes from the ratio of No. 11 (3.0 Yb_2O_3-0.13 Er_2O_3) in Table IV. This table also contains the amount and the price of each material sold on the market.

The total amount of materials used exceeds 5 g so that the weight of the target grass phosphor can be adjusted to 5 g, because Li_2CO_3 causes a chemical reaction and separates into lithium oxide and carbon dioxide while the glass phosphor is being made in the furnace. Hence, the price of the materials for making 5 g of the glass phosphor was approx. 36.82 USD. (The electric bill for furnace operation should be added, but in this paper, we do not include this fee.)

In our previous research [3], we welded approx. 0.05 g of another glass phosphor powder onto the surface of one ceramic plate. Hence, the price of 0.05 g of newly developed glass phosphor is approx. 0.37 USD. This amount of money is less than the cost of a radiofrequency identification (RFID) tag with the same square measurements (from 0.72 to 1.07 USD) in which another glass phosphor powder was welded onto the surface of the ceramic plate. The RFID tag could affect the product's patterns and colors when it adheres to its surface. However, a small amount of glass phosphor powder does not affect the product's patterns and colors because of its transparency and paleness. Hence, the glass phosphor could be categorized as a security product for ceramic products.

We used Er_2O_3 and Yb_2O_3 as rare earth oxides. These materials are easily accessible on the market, and the total percentage of weight compared to the base glass material for making the glass phosphor was low (approx. 13%). In practical use, mass production of the glass phosphor could be expected, so the amount of money spent making the phosphor could be decreased.

V. Conclusion

We made the glass phosphor while changing the

composition of the base glass material and the ratio of the rare earth oxide with the aim of applying multimodal artifact metrics to ceramic products. This glass phosphor has characteristics described in Section 2.A, and its appearance is more transparent and paler than the version used in our previous research. Four types of feature data, described in Section 2.D, could be extracted by welding the powder of the glass phosphor onto the surface of the product during the manufacturing process.

To develop the previously mentioned glass phosphor, we reviewed the composition of the base glass material (in particular, the glass-forming oxide and glass-modifying oxide), because colorless and transparent base glass material was needed. As a result, we found the combination of 75 GeO_2-25 Li_2CO_3 was the best in our experiment. Although the material includes a hygroscopic substance (Li_2CO_3), the material did not become clouded even when it was exposed to the air over 10 months.

To develop transparent and paler glass phosphor using the newly developed base glass material, we made samples by changing the ratio of Er_2O_3 and Yb_2O_3. These samples showed emissions in each light band (red and green, as well as the near-infrared spectrum), and the appearance was transparent and pale pink. Among the samples, the phosphor with the ratio of 3.0 Yb_2O_3-0.13 Er_2O_3 showed the strongest emission in each light band.

The glass phosphor and other materials used (rare earth oxide, glass-forming oxide, and glass-modifying oxide) are safe, and the risk of affecting human health and the environment is quite low. These materials are easily accessible on the market, so the manufacturing cost of making the glass phosphor could be decreased through mass production. In the future, we plan to weld the glass phosphor powder onto the surface of the ceramic product and extract four types of feature data by using a visible and near-infrared camera and spectroscope.

REFERENCES

[1] S. Nakajima, *Nakajima Seinosuke no Yakimono Kantei (Toujiro Books*, Futabasha Publishers Ltd, Japanese, 1996.

[2] T. Matsumoto, "Introduction to artifact-metrocs," *Journal of Printing Science and Technology*, vol. 49, no. 3, pp. 185-189, 2012.

[3] M. Fujikawa, F. Oda, K. Moriyasu, S. Fuchi, and Y. Takeda, "Development of the new artifact-metrics technology for valuable pottery and porcelain products," *Journal of Information Processing*, vol. 55, no. 9, pp. 1992-2007, 2014.

[4] Y. Seto, "Development trends in biometric technology," *Journal of Printing Science and Technology*, vol. 49, no. 3, pp. 190-196, 2012.

[5] M. Fujikawa, K. Jitsukawa, and S. Fuchi, "A study on the multimodal artifact metrics and its application possibility (application for synthetic resin products)," *The Japanese Journal of the Institute of Industrial Applications Engineers*, vol. 5, no. 2, pp. 52-62, 2017.

[6] A. Aoki, T. Ikeda, T. Yamada, Y. Takemura, and T. Matsumoto, "Analysis of document authentication technique using soft magnetic fibers," *The Journal of the Institute of Electrical Engineers of Japan*, vol. 126, no. 5, pp. 269-275, 2006.

[7] K. Okura, "Ganryo no Taikyu Sei," *Journal of the Japan Society of Colour Material*, vol. 46, no. 2, pp. 113-120, 1973.

[8] M. Fujikawa, M. Hara, S. Koyama, and S. Fuchi, "Development of functional material for artifact metrics applicable for ceramics," in *Proc. Multimedia, Distributed, Cooperative, and Mobile Symposium*, 5C-5, 2018, pp. 954-962.

[9] M. Fujikawa, M. Hara, and S. Fuchi, "Development of fuctional materials for multi-modal artifact metrics (#2)," in *Proc. 2019 Symposium on Cryptography and Information Security*, 3D4-4, 2019.

[10] Y. Suzuki, *Popular Science: Kidorui no Hanashi*, Shokabo Co., Ltd., 1998.

[11] Showa Chemical Industry Co., Ltd., *Chemical Substance Safety Data Sheet (Lithium Carbonate)*, SDS No. 12147250.

[12] Junsei Chemical Co., Ltd., *Chemical Substance Safety Data Sheet (Germanium Dioxide).*

Masaki Fujikawa was born on February 6, 1974 in Tokushima Prefecture, Japan. He received his Ph.D. in information engineering from Chuo University, Tokyo, Japan.

He has worked at security service company named ALSOK in Tokyo Japan from 1998 to 2016. During that period, he doubled as a guest researcher of the Research and Development Initiative, Chuo University and the director of an information security R&D project of METI (Ministry of Economy, Trade and Industry, Japan). Now, he is working as an associate professor at Kogakuin University in Tokyo and researching on different security and safety systems in order to build a safer society.

Dr. Fujikawa is a member of IEEE, IPSJ and the steering committee of the IPSJ Computer Security Group. Dr. Fujikawa received a best paper and specially selected paper awards from IPSJ.

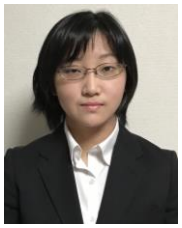

Mariko Hara was born on March 12, 1997 in Kanagawa Prefecture, Japan. Currently, she was an undergraduate student of Faculty of Informatics, Kogakuin University. She was studying about information security systems and physical security systems, such as multimodal artifact metrics and biometrics. She is now with DTS Corporation.

Yasushi Nanai was born on February 26, 1987 in Kanagawa Prefecture, Japan. He received his Ph.D in applied physics from the University of Electro-Communications in 2014. From 2013 to 2015, he was a research fellowship for Young Scientists of Japan Society for the Promotion of Science at the university.

In 2015, he moved to Nihon University as an assistant professor in the Department of Physics in College of Humanities and Sciences. From 2017, he is as an assistant professor in Department of Electrical Engineering and Electronics at Aoyama Gakuin University, Sagamihara, Japan. His work is research and development of rare-earth or 3d transition-metal doped phosphors.

Shingo Fuchi was born in Hyogo Prefecture, Japan, in 1975. He received his master's degree and Ph.D in materials science and engineering from Nagoya University in 1999 and 2002, respectively.

He is an associate professor in the Department of Electrical Engineering and Electronics at Aoyama Gakuin University, Sagamihara, Japan. Before coming to Aoyama Gakuin University, he was a patent examiner at Japan Patent Office, and an assistant professor in the Department of Crystalline Materials Science at Nagoya University. His research interests are semiconductor nano structure, rare-earth doped glasses, and optical device application. he has published over 40 reviewed papers. Dr. Fuchi is a member of JSAP.